

Deflection gating for time-resolved x-ray magnetic circular dichroism—photoemission electron microscopy using synchrotron radiation

C. Wiemann, A. M. Kaiser, S. Cramm, and C. M. Schneider

Citation: [Rev. Sci. Instrum.](#) **83**, 063706 (2012); doi: 10.1063/1.4729603

View online: <http://dx.doi.org/10.1063/1.4729603>

View Table of Contents: <http://rsi.aip.org/resource/1/RSINAK/v83/i6>

Published by the [American Institute of Physics](#).

Additional information on Rev. Sci. Instrum.

Journal Homepage: <http://rsi.aip.org>

Journal Information: http://rsi.aip.org/about/about_the_journal

Top downloads: http://rsi.aip.org/features/most_downloaded

Information for Authors: <http://rsi.aip.org/authors>

ADVERTISEMENT



NEW!

**Hybrid HD-AFM
mode!**

<https://www4.gotomeeting.com/register/984090175>

NT-MDT
Your AFM & Raman Company

Deflection gating for time-resolved x-ray magnetic circular dichroism–photoemission electron microscopy using synchrotron radiation

C. Wiemann,¹ A. M. Kaiser,¹ S. Cramm,¹ and C. M. Schneider^{1,2}

¹*Peter Grünberg Institut PGI-6 “Electronic Properties”, Research Centre Jülich, D-52425 Jülich, Germany*

²*Fakultät für Physik and Center for Nanointegration Duisburg-Essen (CeNIDE), Universität Duisburg-Essen, D-47048 Duisburg, Germany*

(Received 14 December 2011; accepted 31 May 2012; published online 20 June 2012)

In this paper, we present a newly developed gating technique for a time-resolving photoemission microscope. The technique makes use of an electrostatic deflector within the microscope’s electron optical system for fast switching between two electron-optical paths, one of which is used for imaging, while the other is blocked by an aperture stop. The system can be operated with a switching time of 20 ns and shows superior dark current rejection. We report on the application of this new gating technique to exploit the time structure in the injection bunch pattern of the synchrotron radiation source BESSY II at Helmholtz-Zentrum Berlin for time-resolved measurements in the picosecond regime. © 2012 American Institute of Physics. [<http://dx.doi.org/10.1063/1.4729603>]

I. INTRODUCTION

The ongoing progress in nanotechnology and particularly micro- and nanoelectronics requires novel characterization techniques which are able to address both short length and time scales. In this course, several time- and laterally resolved experiments have been developed in recent years and have matured into well-established methods in various fields of research.^{1–6} In general, one may distinguish between scanning and parallel imaging approaches, whereby the latter promise a much faster data acquisition.

Photoemission electron microscopy (PEEM) using electrostatic or electromagnetic immersion lens objectives combines parallel imaging with a particular surface sensitivity.⁷ It has been successfully employed to study the dynamic response of electronic^{8,9} as well as magnetic¹⁰ systems in the framework of pump-probe schemes. These experiments rely on a stroboscopic imaging of repetitive events, which are sampled typically 10^6 – 10^9 times over. The advantage of pump-probe techniques lies in the fact that the time-resolution in the experiment is limited only by the pulse width of the pump and probe pulses. If pulsed laser systems with ultrashort pulses can be employed, a time resolution in the fs-regime is achievable without the need of an explicitly time-resolving detection system.

For the investigation of magnetic systems, the phenomenon of soft x-ray magnetic dichroism (XMCD) in photoabsorption with polarized synchrotron light is exploited to generate a magnetic contrast in PEEM. In ferromagnets, the absorption of circularly polarized x-rays depends on the relative orientation of the helicity vector of the impinging light and the local magnetization direction. Upon light polarization reversal, the magnetic contribution to the total image contrast changes sign, while other contrast mechanisms are not affected. By simple image processing routines like, e.g., division of images taken at opposite helicities, most contrast contributions of other than magnetic origin can be removed and one is left with a map of the local magnetization direction

$\vec{M}(r)$, revealing domain patterns and domain boundaries. By tuning the x-ray source to element-specific absorption lines, chemical selectivity can be achieved. In this way, it is even possible to investigate the magnetic structure of buried layers and interfaces and their temporal development.^{11,12} Using linearly polarized light and exploiting the phenomenon of x-ray magnetic linear dichroism also antiferromagnetic systems may be investigated with respect to domain structures and domain boundaries.^{13–15}

The intrinsically pulsed time structure of the synchrotron light¹⁶ enables a natural use of a pump-probe scheme which can be conveniently employed to investigate the dynamic response of magnetic microstructures to an external excitation, i.e., a magnetic field, a spin-polarized current or a photon field. The pulse width (picosecond scale) and pulse repetition time (nanosecond scale) fits nicely to the relevant time scales for magnetization dynamics. In the approach described below, the excitation (pump) is realized by a short magnetic field pulse, while the system is probed by photoexcitation at element-specific x-ray absorption lines. This type of time resolved XMCD-PEEM is used by a number of groups worldwide.^{17–25} However, the time structure of the synchrotron light dictates the frequency at which the pump-probe cycle can be repeated. This leads to various limitations in the experiments. First, the repetition frequency obviously limits the time the system under investigation is given to relax back into its ground state after excitation (recovery time). Since most synchrotron facilities are operated at repetition frequencies of some hundred MHz, the resulting recovery times are on the order of a few ns. Magnetic systems cover an extremely broad range of time scales for dynamic processes which range from seconds down to picoseconds. Some processes may show a relatively slow response, as for example, domain wall displacements. Depending on the magnetic system, the domain configuration and the magnetic field applied, it may take up to several tens of ns to drive domain walls out of a magnetic element. In an earlier experiment on permalloy

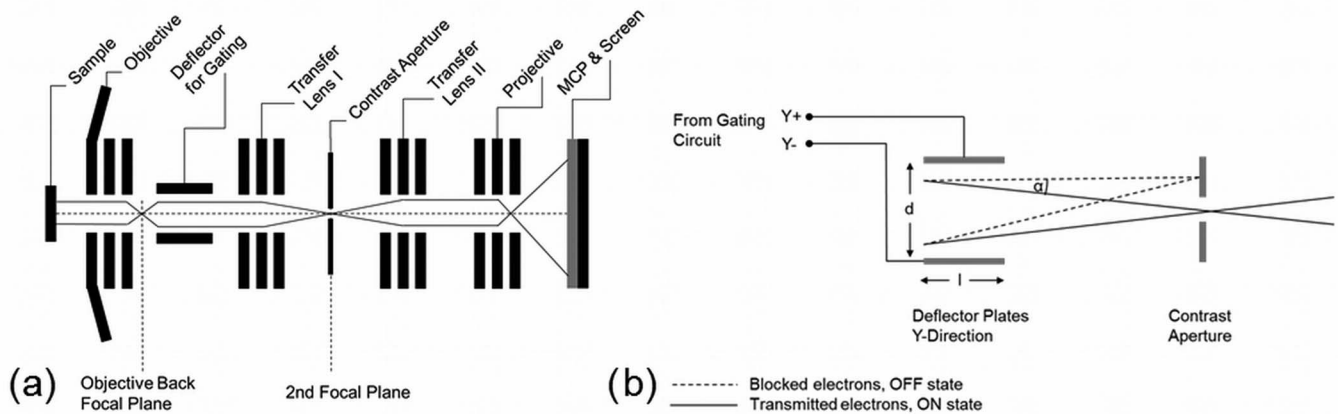


FIG. 1. (a) Sketch of the PEEM lens system. The deflector used for gating is located in the first image plane. The aperture separating the deflected part is located in the second focal plane, behind the first transfer lens. (b) Schematic of the gating operation. Dashed lines: trajectories of electrons while gate is in “OFF” state; solid lines: trajectories of electrons while gate is in “ON” state.

microstructures, we have shown that partial domain walls which are created by incoherent rotation processes of the local magnetization in response to an ultrashort magnetic field pulse, decay on a time scale of 20–30 ns.²⁶ This comes about because the only restoring force available results from the demagnetizing field of the transient domain configuration. Investigations at higher pulse repetition rates will therefore never be able to probe the ground state, but rather some intermediate metastable state.

A second limitation is associated with the generation of the pump-pulse itself. To generate the exciting magnetic field pulse at the sample position, a current pulse running through a nearby single stripline or microcoil loop is commonly employed. These current pulses are desired to be short on the relevant timescale of the magnetic system’s reaction in order to be able to observe the free dynamic response during the return path towards the magnetic ground state. At the same time, they have to have at least a minimum amplitude to induce a sizable displacement from the magnetic ground state in the first place. This results in the demand for high peak currents, which – in combination with the predetermined high repetition frequencies – will lead to an unwanted thermal load on the sample. This is a critical issue especially when investigating materials with a Curie point below room temperature, when sample cooling systems have to be employed.

In order to circumvent these limitations it is desirable to have a tool to reduce the repetition frequency in synchrotron-based pump-probe PEEM experiments. The most straight-forward method to achieve this goal is actually chopping the synchrotron light beam by use of a fast mechanical shutter,²⁷ which is technically very demanding in terms of synchronization and material strength of the chopper wheel. Other ideas include electronically switching the gain of the channelplate (MCP gating) in the PEEM’s imaging system, a concept that has been successfully implemented by some groups,^{28,29} or switching a repeller electrode grid in front of the imaging detector.³⁰

In this paper we present a new gating mechanism that relies on a fast deflection switch which is directly incorporated in the microscope’s electron optics. A similar technique was

already described by Rempfer *et al.*,³¹ although these authors made no comments on the timing performance and did not use it for ultrafast switching applications. We believe that our setup is superior to the MCP gating approach in terms of the achievable switching speed as well as the suppression of dark current and the minimization of heat load on the MCP itself.

II. EXPERIMENTAL DETAILS

The deflection system used for the beam gating is incorporated in the electron optics of a modified electrostatic PEEM instrument from Focus GmbH. Figure 1 shows a schematic view. Electrons emitted from the sample are collected by the objective triode lens and form a slightly magnified ($\sim 40\times$) first real image of the sample surface in the plane of the iris aperture. After passing a transfer lens, the electron beams are focused through a contrast aperture for angle selection. A second transfer lens and a projective lens finally project the further magnified image on the front of a multi-channel plate (MCP), which serves as image intensifier. A fluorescence screen at the MCP output creates a visible image which is in turn recorded by a slow-scan CCD camera system.

The original instrument featured an aperture in the back focal plane of the objective lens in order to reduce angle-dependent image aberrations. In our modified version, the focal plane is projected forward by the first transfer lens to a position further down the optical axis. The contrast aperture has been moved into this second focal plane. The repositioning of the aperture allows for the implementation of the deflection switch, which consists of a pair of deflector plates situated near the first image plane. Charging of the deflector plates results in an electric field perpendicular to the optical axis. Such a field changes electron trajectories near the axis by an additional bending angle

$$\Delta\alpha \approx l\Delta U/2dU_{Col}$$

Here, approximations for small angles have been assumed. While l and d are the linear dimensions of the field region along and perpendicular to the optical axis (see Fig. 1(b)), ΔU is the potential difference between the deflector plates

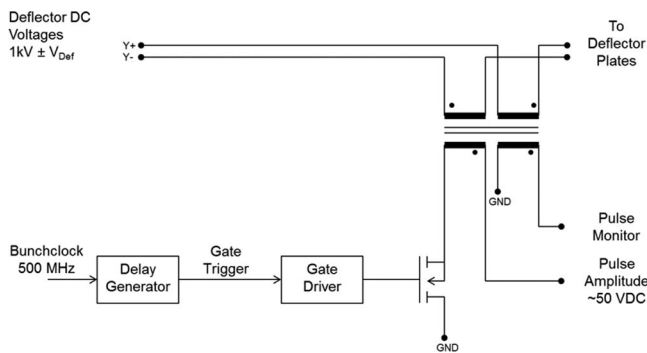


FIG. 2. Schematic of the gating circuit. A trigger signal derived from the synchrotron bunchclock is used to switch a Power-MOSFET, which acts as a variable amplitude pulse generator. The pulse is added by inductive coupling to the DC bias voltages of the deflector.

and U_{Col} is the potential of the microscope column, which determines the velocity of the electrons when entering the field region of the deflector. In the focal plane, an additional deflection angle results in a radial displacement of the electron trajectories, since the phase space coordinates (position and angle) are interchanged with respect to the image plane. To confirm this, simulations of the electron trajectories have been carried out using SIMION 7.³² A linear dependence of the displacement in the focal plane on the applied potential difference at the deflector plates has been found. The gating mechanism works by rapidly toggling the potential of the deflector electrodes between two stable states (Fig. 1(b)). In the “OFF” state, a potential difference of about 100 V between the opposing electrodes deflects the electron trajectories and they are stopped at the plane of the contrast aperture. In the “ON” state, the potential difference is dropped to zero in order to let the electrons pass on the original trajectories through the contrast aperture. To achieve the fast switching of the electrode potentials, the output of a variable amplitude pulse generator is added via inductive coupling to the DC voltage applied to one pair of the deflector plates. Figure 2 shows a schematic of the electronics circuit.

The deflecting pulse is coupled symmetrically, but with opposite sign to both electrodes using two secondary coils of opposite winding sense on the coupler. The DC voltage is used for static beam alignment in the focal plane, while the pulse amplitude can be adjusted to achieve the desired dynamic deflection to spatially separate the trajectories of the electrons in the OFF and ON states. A pulse amplitude of 50 V is sufficient to achieve the desired separation. The variable timing and phase synchronization is realized by a digital delay generator (Highland P400), which is fed by the synchrotron master clock timing signal and delivers a TTL pulse at variable time delay to trigger the pulse generator.

The action of the pulsed deflecting field can be seen in Fig. 3. Here, the second transfer lens has been adjusted in such a way that the focal plane is imaged onto the MCP. The field of view covers $\sim 500 \mu\text{m}$. The timing of the gating window is already positioned around the single bunch in the hybrid bunch operation mode of the synchrotron radiation source BESSY II at Helmholtz-Zentrum Berlin (see below), but a big contrast aperture and a low amplitude of the deflecting pulse has been chosen to image the deflected as well

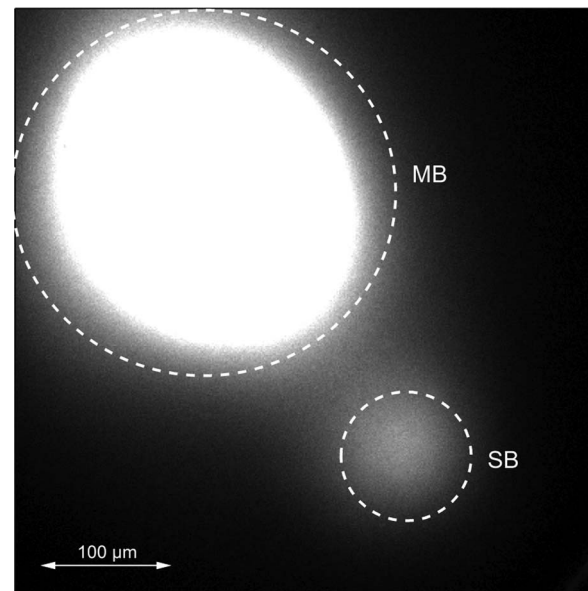


FIG. 3. Spatial separation of multibunch (MB) and singlebunch (SB) contribution of the photoemission signal in the 2nd focal plane.

as the undeflected parts of the beam side by side. Two regions can be discerned: A big bright spot marked “MB” in the upper left containing the deflected part (photoemission signal of the multibunch sequence) and a smaller satellite spot marked “SB” in the lower right, containing the undeflected contribution of the single bunch only. By placing a smaller aperture centered on the smaller focal spot, time-gated imaging using selectively the photoemission from the single bunch can be performed. Since the imaging takes place in the “ON” state while the deflecting field is zero, additional aberrations introduced by the deflector field need not to be taken into account.

III. RESULTS AND DISCUSSION

In order to test the timing performance of the gating setup, the injection pattern of BESSY II was imaged by shifting the gating window versus the storage ring’s 1.25 MHz timing signal marking the single bunch. The ring was operated in the usual hybrid bunch mode, in which $\frac{3}{4}$ of the orbit is filled by a multibunch pattern with 2 ns bunch separation. The remaining $\frac{1}{4}$ of the orbit – corresponding to a time window of about 100 ns – is empty except for a single electron bunch placed in the middle of the empty (dark) zone. Figure 4 shows the resulting photoemission signal integrated over the image detector. At negative delay times, the gating window allows electrons emitted by several bunches of the multibunch sequence to pass. At a time delay of -50 ns, the photoemission signal drops to zero as the window opens only within the dark zone. Around zero delay, only photoelectrons generated by the singular bunch pass the gating window; this is our desired mode of operation. After a subsequent gap, the photoemission signal rises again due to the onset of the multibunch sequence. The 2 ns pulse separation in the multibunch sequence can obviously not be resolved; however, the 100 ns bunch gap and the single bunch within the gap can be clearly distinguished. Taking into account the synchrotron radiation

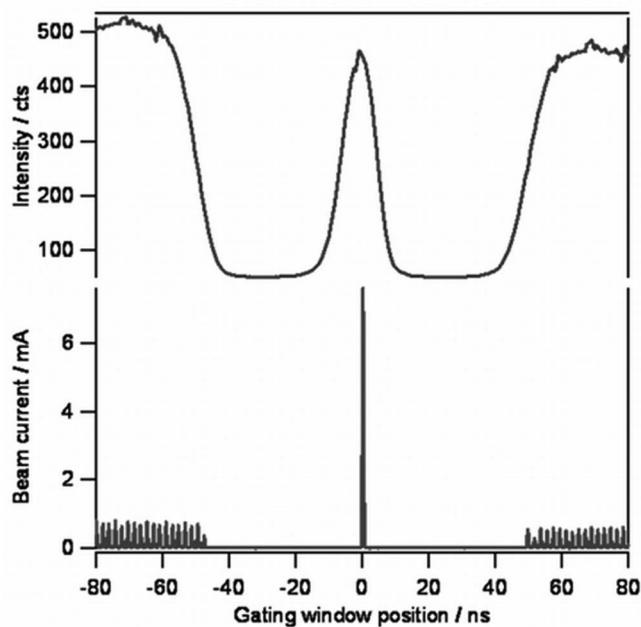


FIG. 4. Integrated photoemission signal (top) vs. gating window position matches the BESSY II injection pattern (bottom).

pulse width (temporal electron bunch width) of 50 ps, we estimate a switching time of about 20 ns for the entire timing circuit in our setup which is comparable to values reported for gating systems based on MCP switching. It also quantitatively matches the RC-time of the deflection plates which show a capacitance of ~ 200 pF. A gated detector employing a channel plate as switching element was already presented by Marconi *et al.*³³ The authors succeeded to switch the operating voltage of a double-MCP assembly by 500 V (corresponding to a voltage drop across each channelplate of about 250 V) with a rise time of 5 ns. However, the detector presented in Marconi's work was not used for imaging applications and achieved an extinction ratio of only 1:100. Quitmann and coworkers re-

ported use of a gated double-stack MCP in a PEEM setup at the Swiss Light Source which is similar to our application.²⁸ They successfully used the gating technique to separate the photoemission signal of a single bunch from a background of regular bunches carrying about 100 times more current. However, while a MCP-Gating setup always shows a finite extinction ratio, the deflection switch used in our approach reliably blocks *all* photoelectrons while in "OFF" state (see Fig. 4).

In order to fully switch off a channel plate, the voltage must be dropped below the gain threshold. A channel plate usually shows an exponentially rising gain dependence on the operating voltage, with voltages ranging between gain threshold around 450 V and breakdown limit around 1100 V. The exact values depend on the plate thickness and the pore diameter. In order to prevent any photoelectrons from being amplified one would therefore have to switch the operating voltage of a single MCP by an amplitude of 500 V, at a capacitance of about 200 pF.³⁴ This is about twice the voltage change as in Marconi's experiment mentioned above. To achieve a performance comparable to that of the deflection switch, we can estimate that the capacitance must be charged and uncharged by a (time-averaged) current in the range of 20 A. We also attempted to use a gating scheme based on MCP switching using the build-in image intensifier unit without any modifications, but the results were not satisfying in terms of switching speed and dark current rejection. Moreover, we experienced heavy crosstalk of the high voltage pulses to other electron-optical elements in the microscope, thereby seriously impairing the image quality. Without going into details we tentatively attribute this behavior to capacitive coupling between MCP and the microscope column, which is connected to the MCP front and at the same time serves as outer electrode for the projective and transfer lenses.

Keeping the gating time window fixed on the single bunch of the hybrid bunch filling pattern, time-resolved XMCD-PEEM experiments can be conducted in much the same way as during the genuine single bunch operation of

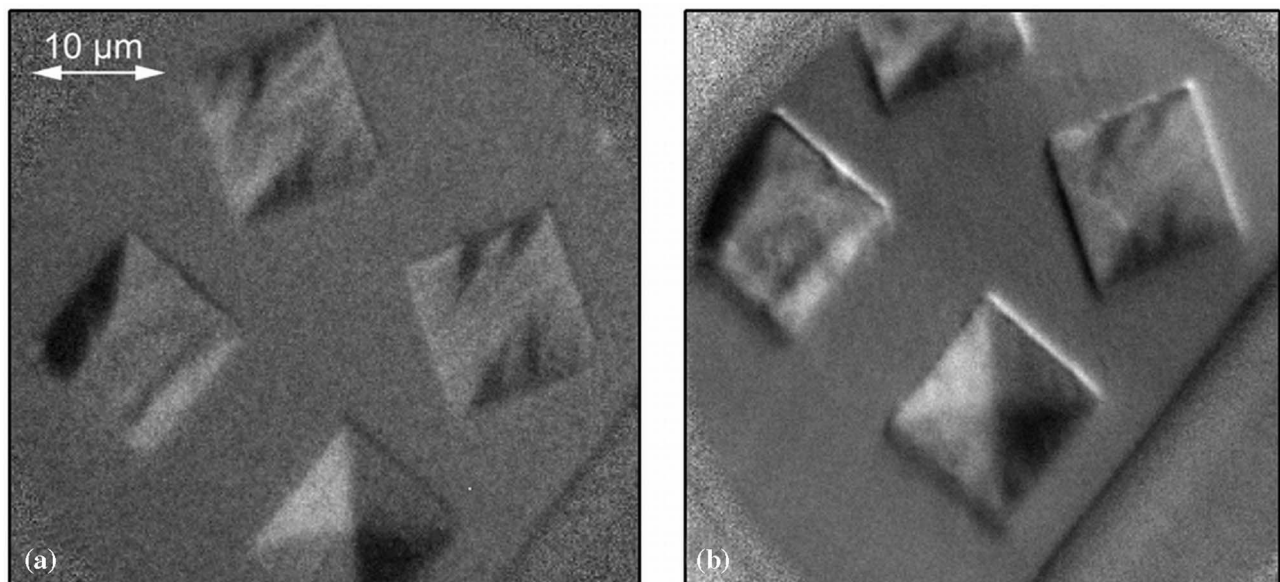


FIG. 5. Comparison of images of magnetic domains, taken during single-bunch operation (a) and gated multi-bunch mode (b), respectively. Both images show calculated asymmetry between images taken at opposite light helicities at Fe L3 edge ($h\nu = 709.25$ eV).

BESSY II. Figure 5 shows a comparison of images taken on the same sample during multibunch operation with gating and during single bunch operation, respectively. Both images are the result of calculating asymmetry between images taken at opposite light helicities at the iron L3 absorption edge. Qualitatively, there is no difference between the images. Note that both images show slight artifacts resulting from sample drift; this is due to the change in thermal load on the sample during switching the undulator from LCP to RCP polarization and has nothing to do with the deflection gating. From a practical point of view the deflection gating in combination with the hybrid bunch filling pattern offers another important advantage. It is much easier to adjust the focus and astigmatism correction of the instrument using the higher photoemission yield generated by the multibunch sequence and then simply switch on the gating for time-resolved measurements. In the genuine single bunch mode with a repetition rate of 1.25 MHz, the photoelectron yield is quite low all the time, which impairs the adjustment of the instrument and leads to long acquisition times for static images. The deflection gating approach ensures a more efficient use of the instrument and a more reliable image quality.

IV. CONCLUSIONS

In conclusion, we have developed a new gating technique for a photoelectron microscope. The technique relies on a fast deflection switch built into the microscope's electron optical system. It enables us to fully exploit the time structure in the hybrid bunch injection pattern of the BESSY II synchrotron for time-resolved experiments, in effect achieving operating conditions for the timing comparable to the genuine single bunch mode. The deflection switch features a switching time of 20 ns and perfect dark current rejection. The technique could easily be incorporated into other electron or ion optical systems to exploit the time structure of other pulsed excitation sources in a similar way, e.g., in experiments relying on pulsed laser sources.

ACKNOWLEDGMENTS

The excellent work of H. Pfeifer and the staff of the electronic workshop in the Peter Grünberg Institut at

Forschungszentrum Jülich is gratefully acknowledged. We also thank K. Grzelakowski for his help in modifying the electron optics of the microscope. This work was partially funded by the DFG within SFB 491.

- ¹M. R. Freeman and A. K. Hiebert, in *Spin Dynamics in Confined Magnetic Structures I*, edited by B. Hillebrands and K. Ounadjela (Springer-Verlag, Berlin, 2002), p. 93.
- ²H. Shigekawa, O. Takeuchi, and M. Aoyama, *Sci. Technol. Adv. Mater.* **6**, 582 (2005).
- ³P. A. Sloan, *J. Phys.: Condens. Matter* **22**, 264001 (2010).
- ⁴H. Dömer and O. Bostanjoglo, *Rev. Sci. Instrum.* **74**, 4369 (2003).
- ⁵D. S. Yang, O. F. Mohammed, and A. H. Zewail, *Proc. Natl. Acad. Sci. U.S.A.* **107**, 14993 (2010).
- ⁶A. Sakdinawat and D. Attwood, *Nat. Photonics* **4**, 840 (2010).
- ⁷S. Hüfner, *Photoelectron Spectroscopy: Principles and Applications* (Springer-Verlag, Berlin, 1995).
- ⁸O. Schmidt *et al.*, *Appl. Phys. B* **74**, 223 (2002).
- ⁹A. Oelsner *et al.*, *J. Electron Spectrosc. Relat. Phenom.* **178**, 317 (2010).
- ¹⁰A. Krasnyuk *et al.*, *Appl. Phys. A: Mater. Sci. Process.* **76**, 863 (2003).
- ¹¹C. M. Schneider *et al.*, *J. Electron Spectrosc. Relat. Phenom.* **181**, 159 (2010).
- ¹²H. Ohldag *et al.*, *Phys. Rev. Lett.* **87**, 247201 (2001).
- ¹³F. Hillebrecht *et al.*, *Phys. Rev. Lett.* **86**, 3419 (2001).
- ¹⁴W. Kuch *et al.*, *Phys. Rev. Lett.* **92**, 017201 (2004).
- ¹⁵F. Nolting *et al.*, *Nature (London)* **405**, 767 (2000).
- ¹⁶D. T. Attwood, *Soft X-rays and Extreme Ultraviolet Radiation: Principles and Applications* (Cambridge University Press, Cambridge, New York, 2007).
- ¹⁷K. Arai *et al.*, *Jpn. J. Appl. Phys.* **50**, 053001 (2011).
- ¹⁸S. B. Choe *et al.*, *Science* **304**, 420 (2004).
- ¹⁹K. Fukumoto *et al.*, *Phys. Rev. Lett.* **96**, 097204 (2006).
- ²⁰W. Kuch *et al.*, *Appl. Phys. Lett.* **85**, 440 (2004).
- ²¹K. Kuepper *et al.*, *Phys. Rev. Lett.* **99**, 167202 (2007).
- ²²N. Ohshima *et al.*, *J. Phys.: Condens. Matter* **23**, 382202 (2011).
- ²³N. Ohshima *et al.*, *J. Appl. Phys.* **107**, 103912 (2010).
- ²⁴J. Raabe *et al.*, *Phys. Rev. Lett.* **94**, 217204 (2005).
- ²⁵J. Vogel *et al.*, *Appl. Phys. A: Mater. Sci. Process.* **92**, 505 (2008).
- ²⁶C. M. Schneider *et al.*, *Appl. Phys. Lett.* **85**, 2562 (2004).
- ²⁷M. Gemmick, and P. Coppens, *J. Synchrotron Radiat.* **14**, 133 (2007).
- ²⁸C. Quitmann *et al.*, *Nucl. Instrum. Methods Phys. Res. A* **588**, 494 (2008).
- ²⁹K. Fukumoto *et al.*, *Rev. Sci. Instrum.* **79**, 063903 (2008).
- ³⁰J. Vogel *et al.*, *Appl. Phys. Lett.* **82**, 2299 (2003).
- ³¹G. F. Rempfer, W. P. Skoczylas, and O. H. Griffith, *Ultramicroscopy* **36**, 196 (1991).
- ³²D. A. Dahl, *Simion 3D V7.0* (Idaho National Engineering Laboratory, Idaho Falls, 1996).
- ³³M. C. Marconi, J. J. Rocca, and G. J. Krauss, *J. Phys. E: Sci. Instrum.* **22**, 849 (1989).
- ³⁴J. L. Wiza, *Nucl. Instrum. Methods* **163**, 587 (1979).